Stereo-SCIDAR system for improvement of adaptive optics space debris-tracking activities

Elliott Thorn, **Visa Korkiakoski**, **Doris Grosse**, **Francis Bennet**, **Francois Rigaut**, **Celine d'Orgeville**, **Josephine Munro**

Research School of Astronomy and Astrophysics, The Australian National University, Canberra, ACT 2611, Australia
Space Environment Research Centre (SERC Limited), Mount Stromlo Observatory, Weston Creek, ACT 2611, Australia

Craig Smith

Electro Optic Systems (EOS), Mount Stromlo Observatory, Weston Creek, ACT 2611, Australia

ABSTRACT

The Research School of Astronomy and Astrophysics (RSAA) in conjunction with the Space Environment Research Centre (SERC) has developed a single detector stereo-SCIDAR (SCIntillation Detection And Ranging) system to characterise atmospheric turbulence. We present the mechanical and optical design, as well as some preliminary results. SERC has a vested interest in space situational awareness (SSA), with a focus on space debris. RSAA is developing adaptive optics (AO) systems to aid in the detection of, ranging to, and orbit propagation of said debris. These AO systems will be directly improved by measurements provided by the usage of the stereo-SCIDAR system developed. SCIDAR is a triangulation technique that utilises a detector to take short exposures of the scintillation pupil patterns of a double star. There is an altitude at which light propagating from these stars passes through the same 'patch' of turbulence in Earth's atmosphere: this patch induces wavefront aberrations that are projected onto different regions of the scintillation pupil patterns. An auto-correlation function is employed to extract the height at which the turbulence was introduced into the wavefronts. Unlike stereo-SCIDAR systems developed by other organisations—which utilise a dedicated detector for each of the pupil images—our system will use a pupil-separating prism and a *single* detector to image both pupils. Using one detector reduces cost as well as design and optical complexity. The system has been installed (in generalised SCIDAR form with a stereo-SCIDAR upgrade scheduled for next year), tested and operated on the EOS Space Systems' 1.8m debris-ranging telescope at Mount Stromlo, Canberra. Specifically, it was designed to observe double stars separated by 5 to 25 arcseconds with a greater magnitude difference tolerance than conventional SCIDAR, that conventional difference being roughly 2.5. We anticipate taking measurements of turbulent layers up to 15km in altitude with a resolution of approximately 1km. Our system will also be sensitive to ground layer atmospheric turbulence. Here we present details of the optical and mechanical design in addition to preliminary results.

Keywords: SCIDAR, generalised stereo-SCIDAR, adaptive optics, atmospheric turbulence

1. INTRODUCTION AND CONCEPT

SCIDAR is a triangulation technique, proposed in 1973 [1], used to characterise atmospheric turbulence: the acronym stands for **sci**ntillation **d**etection **a**nd **r**anging. As light waves travel from distant stars to the surface of the Earth they pass through regions of the atmosphere of differing refractive indices. These differences induce distortions and aberrations into the wavefronts of stars, or any object, that we can observe in space from the Earth see Fig. 1a. This results in the instantaneous brightening and dimming of stars, known as scintillation see Fig. 1b. If we were to observe a pair of targets relatively close together (such as double stars with a small angular separation) the light that reaches our eye from each star will pass through a common region (layer of turbulence) of the atmosphere which is likely to induce wavefront aberrations see Fig. 1c. The aberrations induced by these turbulent layers may then be observed to be projected into the pupil scintillation patterns see Fig. 1d. An auto-correlation function may then be used to extract the height at which the aberration was introduced into the

wavefront, the 'strength' of the turbulence, as well as the wind speed. The only drawback here is that the analysis plane is located at the same altitude as the telescope pupil (primary mirror): the ground layer. This effectively means that the technique is 'blind' to the turbulent ground layer and it has been shown that ground layer turbulence is a significant contributor to telescope performance degradation [2]. A method for moving the analysis plane was proposed [3] whereby the ground layer may be observed: this is known as generalised SCIDAR (GS). Later, a method for separating the pupils was demonstrated [4]: effectively creating a generalised stereo-SCIDAR (GSS) instrument in which each pupil was imaged with a dedicated detector. Separating the pupils allows double stars of a greater difference in magnitude to be observed, increasing sky coverage and sampling of the atmosphere.

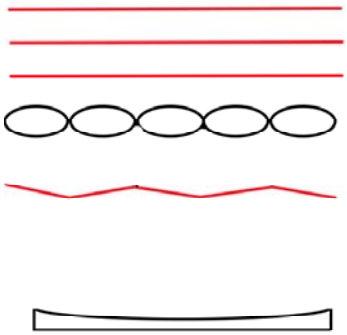

(a) Plane waves (straight) at top before passing through the atmosphere. Black ellipses represent simplified patches of turbulence in atmosphere. Red crinkled line in middle are the aberrated waves after passing through turbulence. Telescope mirror at bottom.

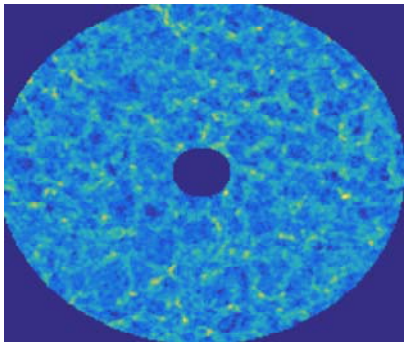

(b) Pupil scintillation pattern on detector. The dark ellipse in the centre is the secondary mirror obscuration.

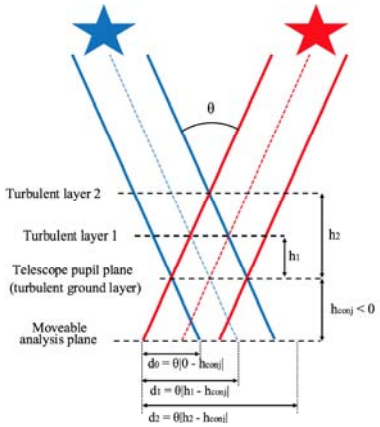

(c) SCIDAR concept illustrated. Note the two different turbulent layers and the locations at which the light from each star 'overlaps' on these layers. It can be seen that the location of a projected aberration in the pupil is related to the angular separation between the stars and the height of the layer under inspection.

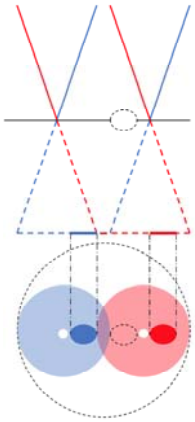

(d) Projected aberrations induced in pupils by a single turbulent cell with which the light from each star interacts. Dashed black lines track the projected aberrations from an edge-on view of the pupils to a plan view. Small black dashed circles represents the turbulent cell. Small white circles represent the obscuration of the secondary in each pupil.

Fig. 1: a) GS mode optical layout, b) GS mode pupil images, c) GSS mode optical layout and d) GSS mode pupil images.

2. SYSTEM REQUIREMENTS, DESCRIPTION AND LAYOUT

The system requirements are reproduced below in Table 1. [5]

The system will be used in the two modes previously mentioned: GS and GSS. Currently, the system is in GS mode and is being used to collect results. A smaller set of acceptable targets is available in this mode, however,

Table 1: System requirements.

Parameter	Requirement
Double star separation	10 - 25 ”
Measurement height, h	At least 15 km
Height resolution, δh	$<$ 1 km
Fried parameter, r_0	5 cm
Conjugate layer propagation distance, h_{conj}	-1 to -3 km
Nominal system wavelength, λ	570 nm
Temporal resolution	Resolve 30 m/s windspeed

we are able to take advantage of the moveable analysis plane. In GSS mode we will be using a compound roof prism to separate the pupils onto a single detector. It is thought that this will reduce cost and system complexity. The physical layout of the system is illustrated in Fig. 2 and annotated items are detailed in Table 2 [5].

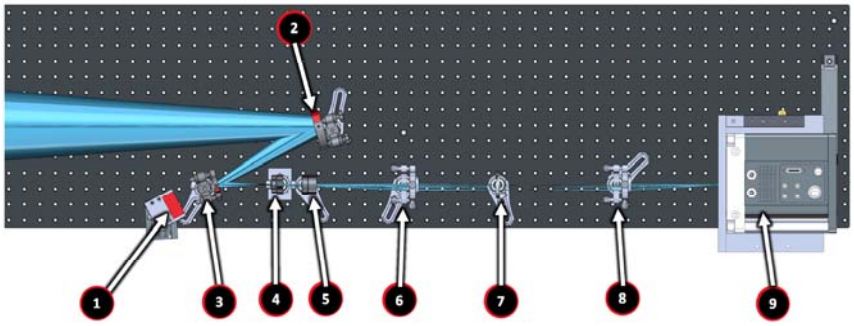

Fig. 2: Mechanical layout of GSS mode. The blue cone at left represents the light path through the system. Table 2 contains annotation descriptions.

Table 2: System components.

Number	Component	Description
1	Acquisition camera	Wide-field USB camera to aid in acquiring targets
2	2” Fold mirror	Folds beam from Coudé lens optical axis
3	1” Dichroic	Folds beam onto imaging camera optical axis, Passes light below λ_{acq} to acquisition camera and light above λ_{acq} to imaging camera
4	Lens one	Collimates beam before passing through prism (prism not shown)
5	Bandpass filter	Allows selection of bandwidth to pass through system
6	Lens two	Lens two and lens three act as a relay
7	Field stop	Prevents stray light from reaching the detector
8	Lens three	Collimates beam to allow imaging of pupil and part of a relay with lens two
9	Imaging camera	OCAM2K (Hnu Nuvu 128 pictured) (PCO Edge 4.2 in GSS mode)

Further details of the system layout and component functionalities may be reviewed in previous papers [5] and [6].

3. PRELIMINARY RESULTS

Thus far we have conducted two observation runs generating results for both. The first run (first light) was mainly concerned with evaluating system performance and fine-tuning. Some results were gathered, but these were largely unusable, see Fig. 3a and Fig. 3b. The instantaneous pupil image shown in Fig. 3a appears elliptical as opposed to circular: this suggests misalignment either of the system itself or elements within the coude path or potentially both. There also appears to be some vignetting present, note the drop-off of illumination around the edges of the pupil.

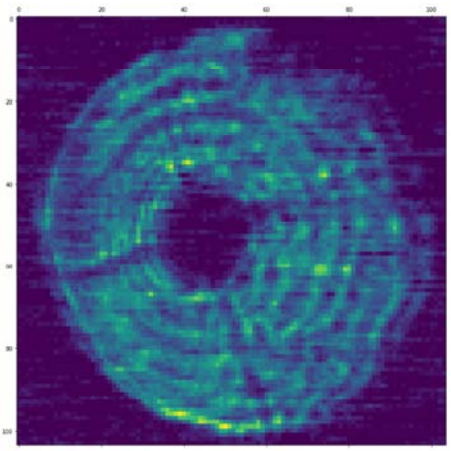

(a) Instantaneous pupil image of first results run. Note the horizontal noise in the image. It is not clear what the source of this noise is, and auto-correlating this pupil image results in the image shown at right.

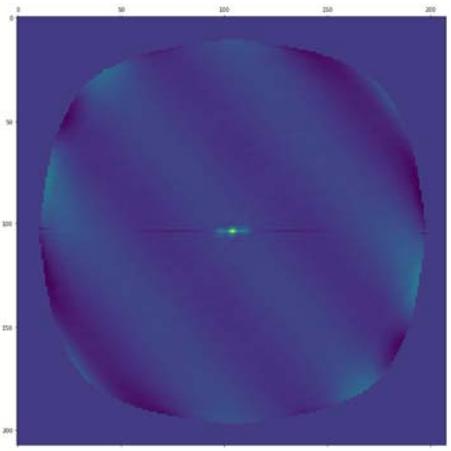

(b) Auto-correlation of instantaneous pupil image shown at left. This does not match expectations at all. It is thought that the noise is at least partly responsible for this.

Fig. 3: Unusable results generated during first results run. At left is a noisy instantaneous pupil image. At right is a corrupted auto-correlation of the aforementioned instantaneous pupil image.

A second set of results collected approximately one month later were more interesting. Two double stars were observed and layers may be seen (more clearly in the two data sets to the far right) in Fig. 5 at altitudes of 1km (a single thin layer), 5-7 km (perhaps one to two layers) and 12-15 km (two well-defined layers). The ground layer is unresolved due to a very low conjugation altitude. The different data sets collected were for the targets tabulated, Table 3. It is fairly easy to distinguish between the first target and the second (the first target was of a higher magnitude than the second target) although the layers observed utilising the dimmer double star are still resolved, particularly the higher layers between 12 and 15 kilometres. For these measurements an r_0 of between 0.3 and 0.4 at 500 nm is estimated. This estimation of course does not take the ground layer into account (as it was unresolved). Expectations assumed that r_0 above Mt. Stromlo would take the value of approximately 0.1 m. As the ground layer is ignored this could suggest that the actual value of r_0 is being overestimated. Further observations are required, paying particular attention to conjugating the detector to an altitude whereby the ground layer can definitely be resolved. Observe also that resolution is finer for the second target: the target with the greater angular separation. Recall that the resolution is defined by Equation 1, [4].

$$\delta h(z) = 0.78\frac{\sqrt{\lambda z}}{\theta} \tag{1}$$

Where: λ is the wavelength of interest, z is the propagation distance to the layer under examination, and θ is the angular separation between the stars. Fig. 4a shows an averaged pupil image with some artefacts: we are investigating vignetting in the coude path as a potential cause. Fig. 4b shows an auto-correlation of a dataset: note that two layers are visible. Fig. 4c shows a spatio-temporal cross-correlation that matches well with theoretical expectations (three frames time difference at 250 Hz), again the two layers stand out with a potential low-altitude layer near the centre of the image.

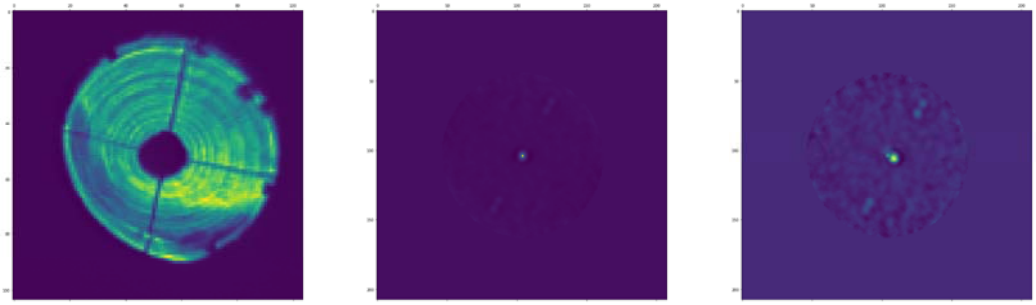

(a) Averaged pupil image with artefacting around the edges.

(b) Auto-correlation of averaged pupil images.

(c) Spatio-temporal cross-correlation (time difference is three frames at 250 Hz).

Fig. 4: Collection of results including: Fig. 4a showing an averaged pupil image, Fig. 4b auto-correlated pupil image, and Fig. 4c spatio-temporal cross correlation.

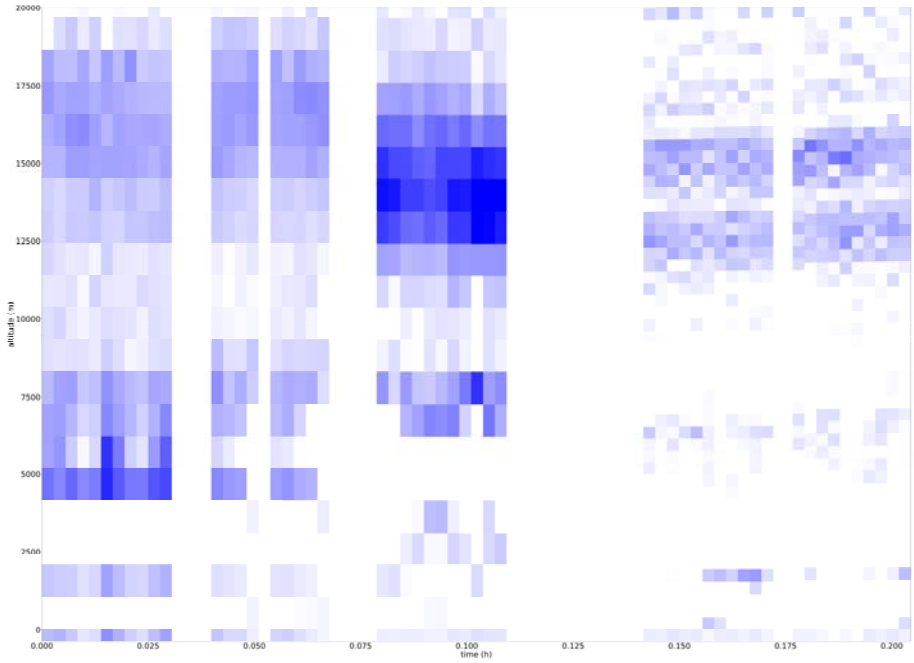

Fig. 5: Strength of turbulence: altitude in metres on y-axis, and time in hours on x-axis. Note that the time axis is not to scale: time was needed to search for the targets, record bias frames and conjugate to the altitude under inspection. The white vertical spaces in between data sets are periods where no data was collecetd: i.e. time spent looking for targets, recording bias frame etc. The three blocks to the left represent the 3.9" separated double star, and the two blocks to the right represent the 10.2" separated referred to in Table 3.

Table 3: Target data collection.

Magnitude	Magnitude	Separation [arcsec]	Imaging rate [Hz]	Conjugation
1.25	1.65	3.9	250	To ground
1.25	1.65	3.9	250	To ground
1.25	1.65	3.9	250	To small negative altitude
5.1	5.6	10.2	250	To small negative altitude
5.1	5.6	10.2	250	To small negative altitude

4. CURRENT STATE OF THE PROJECT

The system has been completed and is currently being used in GS mode to gather preliminary results. We are awaiting quotations on the pupil-separating prism and are conducting mechanical design of the prism mount—with an aim to update the system to GSS mode. Simulation work was conducted earlier in the year to gain an understanding of the types of artefacts and limitations that may arise when analysing actual recorded data. Some of the issues discovered include: false positive layer detection, failure to detect exisiting layers, and falsely identifying a single layer as a cluster of multiple individual layers. False positive layer detection occurred when adjusting the recorded data noise threshold: however most of these were safely ignored as they indicated a negative altitude. Another issue is loss of signal due to turbulent *boiling*. This boiling effectively causes diffusion of light and ultimately a reduction in signal received by the detector. It is not understood to what extent (if at all) turbulent boiling affects the results.

5. CONCLUSION

We have gathered generalised SCIDAR results using a SCIDAR instrument designed and operated by the RSAA in conjunction with SERC. It has been shown that our system is capable of identifying turbulent atmospheric layers up to an altitude of 15km satisfying one of the original requirements. We are currently operating the system in generalised SCIDAR mode but will be upgrading to a stereo-SCIDAR system next year utilising a pupil-separating prism, allowing us to resolve the turbulent ground layer. Our stereo-SCIDAR system will utilise a single detector saving on cost.

ACKNOWLEDGEMENTS

The authors would like to acknowledge the support of the Cooperative Research Centre for Space Environment Management (SERC Limited) through the Australian Government's Cooperative Research Centre Programme. This research is supported by an Australian Government Research Training Program (RTP) scholarship.

REFERENCES

[1] J Vernin and F Roddier. Experimental determination of two-dimensional spatiotemporal power spectra of stellar light scintillation evidence for a multilayer structure of the air turbulence in the upper troposphere. *JOSA*, 63(3):270–273, 1973.

[2] F Roddier, L Cowie, J Elon Graves, A Songaila, and D McKenna. Seeing at mauna kea-a joint uh-un-noao-cfht study. In *Advanced Technology Optical Telescopes IV*, volume 1236, pages 485–491, 1990.

[3] A Fuchs, M Tallon, and J Vernin. Focusing on a turbulent layer: principle of the generalized scidar. *Publications of the Astronomical Society of the Pacific*, 110(743):86, 1998.

[4] J Osborn, RW Wilson, T Butterley, R Avila, VS Dhillon, TJ Morris, and HW Shepherd. Stereo scidar: Profiling atmospheric optical turbulence with improved altitude resolution. 2013.

[5] E Thorn, D Grosse, F Rigaut, and F Bennet. Site testing for space situational awareness with single-detector stereo-scidar. In *Advanced Maui Optical and Space Surveillance Technologies Conference*, 2016.

[6] Doris Grosse, Francis Bennet, Visa Korkiakoski, Francois Rigaut, and Elliott Thorn. Single detector stereo-scidar for mount stromlo. In *SPIE Astronomical Telescopes+ Instrumentation*, pages 99093D–99093D. International Society for Optics and Photonics, 2016.